NEAR-SURFACE GEOTHERMAL MAPPING – TESTING THE tTEM GEOPHYSICAL TECHNIQUE IN THE ROTORUA GEOTHERMAL FIELD

Robert Reeves[1], Jesper Pedersen[2], Thomas Brakenrig[1], Pradip Maurya[2], Rune Kraghede[2], Frederik Christenson[2], Liam McGovern[1] and Brian Moorhead[3]

[1] GNS Science, 114 Karetoto Road, RD4, Taupō 3384, New Zealand

[2] Aarhus University, Nordre Ringgade 1, 8000 Aarhus, Denmark

[3] Lincoln Agritech, Ruakura Research Centre, Ruakura Lane, Hamilton 3214, New Zealand

r.reeves@gns.cri.nz

Keywords: *Rotorua geothermal Field, tTEM, Geophysics, permeability, resistivity, geothermal mapping*.

ABSTRACT

The towed transient electromagnetic (tTEM) geophysical technique enables high-resolution near-surface resistivity measurements to be collected in a timely manner, resulting in a better understanding of the near surface (approx. top 100 m). The tTEM system in development by Aarhus University is tested in the Rotorua Geothermal Field, New Zealand. The aims of the work are to test the equipment in a low-resistivity environment where abrupt changes in resistivity may occur over short distances and to better define subsurface areas of geothermal activity and provide insights into the permeability structure between the groundwater aquifers and geothermal surface features.

tTEM data collected from two sites show that the tTEM method can successfully define shallow resistivity targets and provide insights into the near-surface permeability structure. Areas of low resistivity correlate well with mapped geothermal surface features and suggest that subsurface areas of geothermal influence are larger than what is seen at the surface.

A large amount of the tTEM data collected in part of the study had to be discarded because they were of poor quality – probably affected by cultural effects such as electric power lines and buried objects. However, the poor data was largely constrained to one part of the study area, so a good resistivity model could be generated in other parts of the study area and achieve the projects aims.

1. INTRODUCTION

There is an increasing need to image the top 100 m of the subsurface using geophysical techniques. Industries that are demanding detailed imaging include geotechnical, infrastructure, groundwater, geothermal, environmental, mineral resources and hazards. Geophysical surveys for these industries inform studies that can have major implications on resource use, resource protection, regulatory and policy development and community resilience.

A large range of geophysical techniques can be used to interpret near-surface geology. Selection of technique will depend on the target, depth and type of geology. Ground-penetrating radar, resistivity / electrical resistivity tomography, transient electromagnetics, seismic reflection/ refraction, magnetics and gravity/microgravity are all examples of established and proven geophysical techniques to investigate the subsurface. Towed TEM (tTEM) is a relatively new electromagnetic geophysical technique that has the advantage over traditional methods in that it enables large quantities of data to be collected quickly and efficiently, thus enabling detailed mapping of shallow targets.

Resistivity techniques have been very successful in mapping high-temperature geothermal areas where there are strong contrasts in resistivity between the country rock and the geothermal system (e.g. Bibby et al. 1994; Spichak and Manzella 2009; Hersir et al. 2020). The strong resistivity contrasts in geothermal areas are generally caused by low-resistivity materials (such as hydrothermally altered rocks and/or strata containing high-salinity fluids) with the higher-resistivity country rocks.

Geothermal areas present unique geological conditions that offer development opportunities in potentially hazardous environments. Having a clear understanding of the geothermal resource will inform decisions related to development potential and include factors such as resource availability, potential environmental effects of a development and geothermal hazards. Types of hazards associated with geothermal activity can include gas (H_2S, CO_2), heat (hot water/steam), ground subsidence, formation of collapse holes and hydrothermal eruptions. Resolving permeable pathways of geothermal fluids to the surface will improve resource and hazard assessments of geothermal areas.

This paper presents preliminary results of a tTEM survey at a site in the Rotorua Geothermal Field, New Zealand. The objective of the survey is to test how the tTEM method performs in a geothermal setting and if new insights into the near-surface geothermal permeable environment can be obtained.

2. STUDY AREA

Rotorua is located in the central part of the North Island of New Zealand (Figure 1). Rotorua city lies at the southern end of Lake Rotorua and has a population of approximately 72,500. Geothermal activity in Rotorua, and the eastern side of Lake Rotorua, has been well documented (e.g. Allis and Lumb 1992; Gordon et al. 2005; Scott et al. 2016). There are over 1500 mapped surface

ISSN 2703-4275

geothermal features that include hot ground, springs, pools, geysers and mud features. The geothermal resource is highly valued for its cultural and tourist values and is utilised for domestic and commercial purposes using shallow (<250 m deep) bores.

Rotorua city lies at the southern end of the Rotorua caldera – a roughly 15-km-wide circular in-filled depression that formed about 140 ka following the volcanic eruption of the Mamaku Ignimbrite (Wood 1992). Several rhyolite domes (and flows) clustered at the southern end of the caldera have formed post-caldera collapse. Sediments, lacustrine sediments and tephras (Rotorua Basin Sediments) have been filling the basin since the caldera collapse. The Rotorua Basin Sediments are described as layered sequences of mixed primary and redeposited tephra, alluvium and lacustrine sediments (and include pumice sands and gravels, muddy lithic breccias, carbonaceous siltstones, peat beds and diatomite) known to be up to 235 m thick (Wood 1992).

Variations in water level over the last 140 ka within the caldera has seen sediments deposited up to 90 m above the current water level of the lake and several terraces form around the edges of the caldera. The sediments generally cover the Mamaku Ignimbrite within the caldera and, in some cases, also cover some of the rhyolite domes. Numerous faults within the Rotorua caldera have been proposed (e.g. Wood 1992, Taylor and Stewart 1987, Milner et al. 2002); however, sediment cover within the caldera results in little or no surface expression and thus confirming the presence of faults within the caldera is difficult.

The Rotorua Geothermal Field underlies part of Rotorua city. Its spatial extent is estimated to be between 18 and 28 km^2, based on the resistivity boundary (Bibby et al. 1992). Deep geothermal fluids rise along the eastern and southern parts of the system and divide into three shallow up-flow zones within the geothermal field (Giggenbach and Glover 1992). Fluids disperse within the local geology (which include the sediments, faults and buried rhyolite domes) from within these areas to create a range of unique hydrological environments and surface geothermal features.

The Puarenga Park study area lies close to the eastern boundary of the Rotorua Geothermal Field. It is characterised by large open areas (sports park, horse racing course) and geothermal activity in an urban area (Figure 1). Surface geothermal activity includes sinter, heated ground, hot pools and weakly steaming ground. The northern part of the area is bounded by Lake Rotorua, and is known as 'Sulphur Flats' – an area of strong geothermal activity that includes discharging springs, steaming ground, sinter and hot pools. Publicly accessible walking tracks through 'Sulphur Flats' allow access to this area. The Puarenga study area was one of two areas selected in Rotorua because of accessibility, closeness to geothermal surface features and the presence of relatively large flat areas to conduct the tTEM survey.

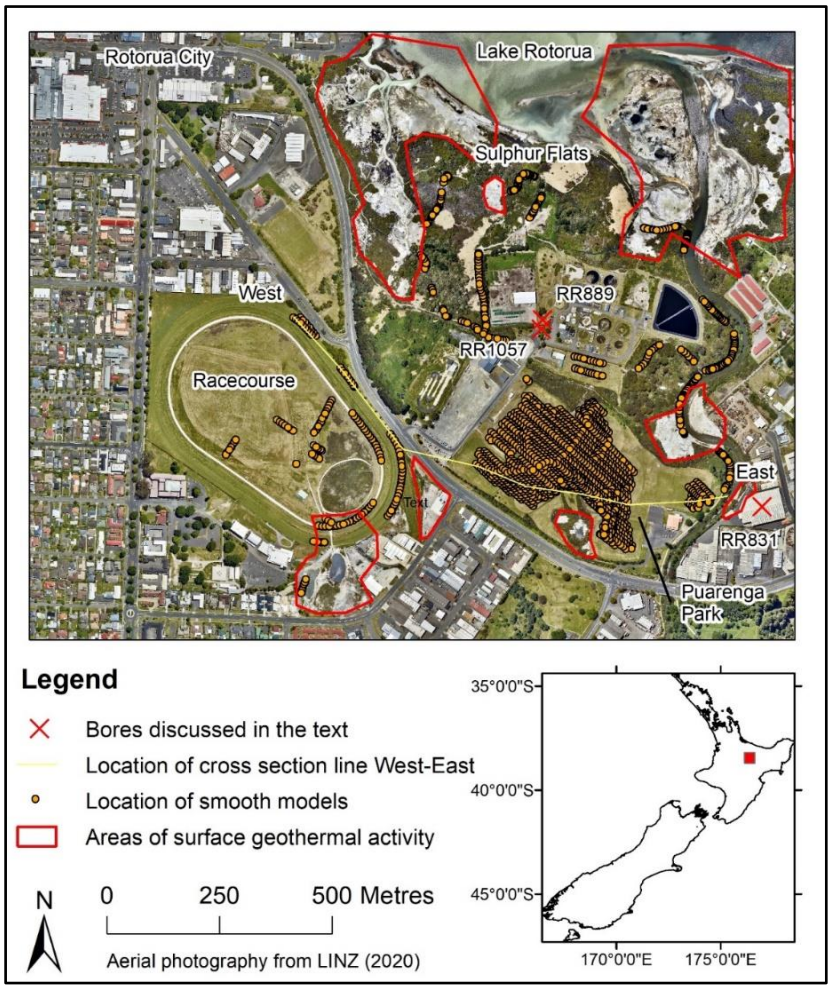

Figure 1: The study area with locations of tTEM smooth models, wells, cross-section and geothermal surface features. The red box in the insert shows the location of the study area in New Zealand.

ISSN 2703-4275

3. METHOD

The tTEM equipment (described in detail in Auken et al. 2018) is installed on a quad bike towing two sleds that use an offset TEM configuration between the receiver and the transmitter. The system collects data by automatic triggering of the system approximately every 2 seconds while towing the equipment at speeds up to 15 km/hr, resulting in a measurement approximately every 4 m. The equipment is towed in lines along existing tracks or where safe access is permitted within the study area. Data is recorded using a dual moment system that stacks data to minimise the noise to signal ratio. Table 1 summarises key specifications of the tTEM system. The equipment has an on-board GPS that recorded the locations of the measurements in real time.

Data were collected between 7/12/20 and 9/12/20 in the Puarenga study area.

Table 1: Key tTEM system specifications.

	Low moment (LM)	High moment (HM)
Transmitter area (single turn)	8 m^2	8 m^2
Tx current	~2.8 A	~30 A
Tx peak moment	~22.4 Am^2	~240 Am^2
Pulse repetition frequency (50 Hz power line frequency)	2110 Hz	660 Hz
Number of pulses/time	422/0.20 s	264/0.40 s
Duty cycle	42%	30%
Tx on-time	200 µs	450 µs
Turn-off time	2.5 µs	4.0 µs
Gate time interval (from beginning of turn-off)	4–33 µs	10–900 µs
Number of gates	15	23

Data are processed and inverted using the tTEM module of the Aarhus Workbench software.

Coupled and anomalous data are identified and removed using both automated and manual methods. Averaging of data using trapezoid filters also enhances data quality, particularly at later time gates, and provides estimates of data uncertainties. A 1D resistivity model is generated by inverting the data for each averaged sounding (see below).

The inversion of the averaged tTEM data is performed with spatially constrained (SCI) 1D smooth models (Viezzoli et al. 2009), forming pseudo 3D model spaces. The inversion algorithm includes modelling of all the key parameters of the system transfer function, such as transmitter waveform, transmitter/receiver timing, low-pass filters, gate widths and system geometry. Data are checked for anomalies and then re-processed.

Note that the SCI model for the Puarenga area also uses tTEM data collected from the Arikikapakapa study area (located approximately 2 km southwest of the Puarenga study area) that is not presented in this paper. This is not expected to make a difference to the key findings in this paper.

Two quality control parameters calculated by Workbench as part of the modelling calculations are presented and discussed:

1) A ‘Standard Depth of Investigation’ (DOI) (Christiansen and Auken 2012) is calculated for each resistivity model that provides an estimated depth to the reliability of the data. Resistivity models below the Standard DOI are generally poorly represented in the data and are discarded (seen in the cross-section by blanking models out below this depth).

2) Data residuals – the data residual expresses how well the obtained resistivity models fit the recorded data. The data residual values are normalised with the data standard deviation, so a data residual below one corresponds to a fit within one standard deviation.

Visualisation of resistivity with depth is achieved using a cross-section designed to span the study area, include as many models as possible, intersect areas of geothermal surface features and be relatively close to other datasets (such as bores) to enable comparisons between bore data and the cross-section. Resistivities below the DOI in the cross-section have been blanked.

4. RESULTS AND DISCUSSION

A SCI resistivity model was successfully generated for the study area. Most of the data from the racecourse (Figure 1) was not used due to poor data quality. Poor data quality in this area is probably caused by buried objects and racecourse infrastructure. Good data was obtained from the Puarenga Park and small sections of the racecourse (see locations of smooth models, Figure 1). Resistivity model fits to the tTEM data were good, with data residuals ranging from 0.17 to 2.3 and with approximately 90% of the models having data residuals of 1 or less.

The study area is generally electrically conductive, with modelled resistivities ranging from approximately 1 Ωm to 200 Ωm. Low resistivities in the study are expected, given the geothermal alteration (causing low-resistivity clays), high-salinity geothermal fluids

ISSN 2703-4275

and the sedimentary characteristics of the near-surface geology. The conductive nature of the study area limits the tTEM signal penetration, resulting in a typical DOI of approximately 50 m (although this depends on the tTEM data and resistivity structure at each sounding).

Figure 2 shows a resistivity cross-section along profile West–East (Figure 1) correlated with other datasets. Key features of the cross-section include relatively high resistivities near the surface; two distinct low-resistivity anomalies with relatively sharp boundaries located approximately 50 m below the ground; and some 'layering' of resistivities, suggesting some lateral features. These are discussed below.

Confidence in the resistivity model is high, given the good correlation with other datasets. The cross-section (Figure 2) is compared to modelled temperature contours (Ratouis et al. 2017), down-hole temperature profiles of wells RRF1057 and RRF831 (measured in 2019 and 2002, respectively) (Figure 1) (Alcaraz 2014), geology (Wood 1992), faults (Lamarche 1992) and the locations of geothermal surface features / warm ground (Reeves et al. 2014, Thompson 1971). We assume that down-hole conditions (temperatures and geology) for wells projected onto the cross-section are representative of conditions on the cross-section.

Key observations comparing the resistivity cross-section with the other datasets (Figure 2) and their interpretation (Figure 3) include:

1) High resistivities near the surface are consistent with the 'Pumice sands and Tephra' geology from Bore RRF889. Areas of thinning of this layer can be inferred from the cross-section. An approximately 10–30 Ωm resistivity zone on the eastern side of the cross-section is consistent with the location and thickness of the 'Muddy pumiceous sands and gravel' unit identified in Bore RRF889. This layer has a relatively sharp vertical resistivity boundary on the edge of the eastern low-resistivity anomaly (Anomaly B, Figure 2). This could be due to a change in geology and/or geothermal alteration.

2) The two areas of very low resistivity (Anomalies A and B, Figures 2 and 3) are consistent with zones where temperature contours indicate higher temperatures closer to the surface. The two zones also are associated with modelled temperatures of between 80 and 100°C. These two areas are interpreted to be caused by clays caused by hydrothermal alteration and could represent localised up-flows of geothermal fluids. Anomaly B has a 'dome' shape analogous to the clay caps seen in high-temperature geothermal reservoirs. Anomaly A has more of a 'flatter top', which may be the result of higher lateral permeability in this area compared to the area around Anomaly B.

3) The temperature profile at bore RRF1057 shows warm water (approx. 50°C) below the upper geological layer, and that water temperature is relatively constant to approximately 230 m elevation, then increases to above 100°C. The temperature increase coincides with the location of Anomaly B. This indicates that water in the area is geothermally influenced and that two-phase conditions can exist at Anomaly B.

4) The elevation of the top of Anomaly B coincides with the elevation of the upper boundary of the sandy siltstone layer. This suggests a possible geological constraint for the shallow part of the geothermal reservoir in this area.

5) The bottom of Anomaly B is inferred to coincide with the top of a fault identified by seismic refraction survey (Lamarche 1992). This relationship is inferred because the top of the fault lies in a zone below the DOI of the resistivity model and therefore the resistivity data cannot be relied on at this depth. However, given that the difference between the bottom of the resistivity model and the top of the fault is approximately 10 m, we believe this interpretation is valid. This also probably falls within the location errors of both the fault and the resistivity data. The fault provides a possible mechanism for geothermal fluid to flow from depth into this anomaly.

6) There are resistivity variations (both vertical and lateral) within the 'Muddy pumiceous sands and gravels' geological layer. This may reflect variations in geological compositions but can also provide some insights into lateral flows of the groundwater / geothermal fluids. An approximately 6 Ωm layer extending from the top of Anomaly A to the east at about 270 m elevation could represent an aquifer that enables lateral flow of geothermal fluids and then, eventually, to the surface, given that this layer is close to an area of geothermal surface features. There is some uncertainty about this given that there is a data gap in this area.

7) Geothermal surface features are generally above, or close to, the edges of the low-resistivity anomalies. Potential feed zones to the geothermal surface features are proposed in Figure 3.

ISSN 2703-4275

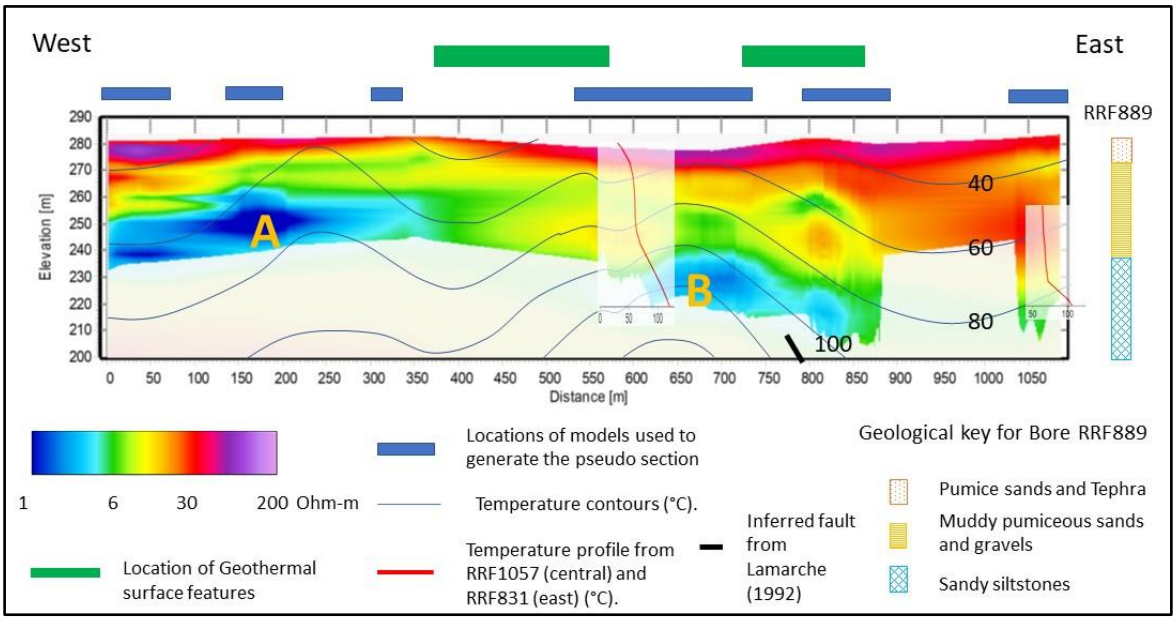

Figure 1: Cross-section West–East showing the resistivity model with other existing data.

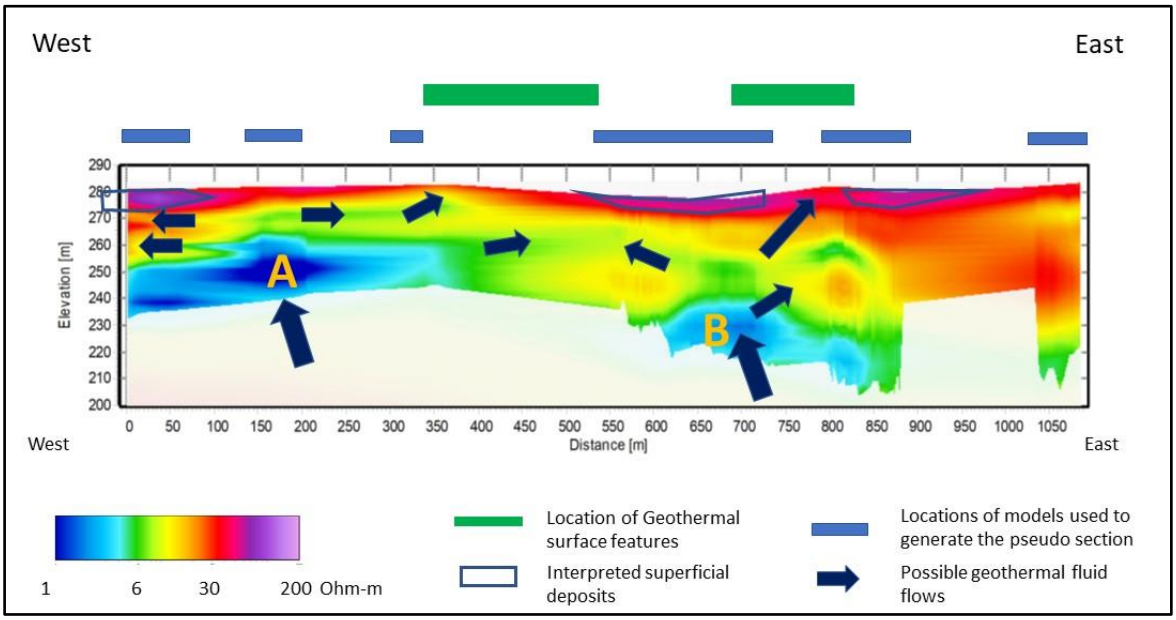

Figure 2: Cross-section West–East with possible geothermal fluid pathways.

5. CONCLUSION

The tTEM system developed by Aarhus University was tested at a geothermal site in Rotorua, New Zealand. Resistivity models inverted from the tTEM data show that the study area was generally electrically conductive as would be expected in a geothermal environment. Two modelled low-resistivity anomalies at approximately 30–40 m depth were resolved and corelated well with existing geological, groundwater temperature and faulting information in the area. Numerous potential geothermal fluid pathways to the surface are identified from the resistivity data.

The findings of this work provide confidence that the tTEM system, in combination with the processing and modelling techniques, works well in geothermal areas for shallow (<100 m depth) areas of interest. However, tTEM data quality is very susceptible to buried objects and other man-made objects, and caution should be used when selecting sites to be surveyed, particularly in urban environments.

ACKNOWLEDGEMENTS

The authors would like to thank Rotorua District Council and Rotorua Racing Club for allowing access to the study areas. We would also like to thank Graham Gusman for allowing us to store the equipment in his workshop while the equipment was in Rotorua. This project was funded through the GNS Science Large Project Infrastructure Fund (LPIF) and the New Geothermal Futures SSIF programme.

REFERENCES

Alcaraz, S.A.: *A 3-D model of the Rotorua Geothermal Field, data inventory and data validation*. Wairakei (NZ): GNS Science. Consultancy Report 2014/276. 29 p. + 1 disc. Prepared for Bay of Plenty Regional Council

Allis, R.G. and Lumb, J.T.: The Rotorua geothermal field, New Zealand: Its physical setting, hydrology, and response to exploitation. *Geothermics, 21 (1–2).* pp. 7–24. https://doi.org/10.1016/0375-6505(92)90065-H. (1992).

Auken, E., Foged, N., Larsen, J.J., Lassen, K.V.T, Maurya, P.K., Dath, S.M., Eiskjær, T.T.: tTEM – A towed transient electromagnetic system for detailed 3D imaging of the top 70 m of the subsurface. *Geophysics, 84 (1).* pp. E13–E22. https://doi.org/10.1190/geo2018-0355.1. (2018).

Bibby, H.M., Bennie, S.L., Stagpoole, V.M., Caldwell, T.G. Resistivity structure of the Waimangu, Waiotapu, Waikite and Reporoa geothermal areas, New Zealand. *Geothermics, 23 (5–6).* pp 445–471. https://doi.org/10.1016/0375-6505(94)90013-2. (1994).

Bibby, H.M., Dawson, G.B., Rayner, H.H., Bennie, S.L., Bromley, C.J.: Electrical resistivity and magnetic investigations of the geothermal systems in the Rotorua area, New Zealand. *Geothermics, 21 (1–2).* pp. 43–64; https://doi.org/10.1016/0375-6505(92)90067-J. (1992).

Christiansen, A.V. and Auken, E.: A Global Measure for Depth of Investigation. *Geophysics, 77 (4).* pp. WB171–WB177. https://doi.org/10.1190/geo2011-0393.1. (2012).

Giggenbach, W.F. and Glover, R.B.: Tectonic regime and major processes governing the chemistry of water and gas discharges from the Rotorua geothermal field, New Zealand. *Geothermics, 21 (1–2).* pp 121–140. https://doi.org/10.1016/0375-6505(92)90073-I. (1992).

Gordon, D.A., Scott, B.J., Mroczek, E.K., compilers: *Rotorua Geothermal Field management monitoring update: 2005*. Whakatane (NZ): Environment Bay of Plenty. (Environmental publication; 2005/12). (2005).

Hersir, G.P., Árnason, K., Vilhjálmsson, A.M., Saemundsson, K., Ágústsdóttir, Þ., Friðleifsson, G.O.: Krýsuvík high temperature geothermal area in SW Iceland: Geological setting and 3D inversion of magnetotelluric (MT) resistivity data. *Journal of Volcanology and Geothermal Research, 391*. pp. 106500. https://doi.org/10.1016/j.jvolgeores.2018.11.021. (2020).

Lamarche, G.: Seismic reflection survey in the geothermal field of the Rotorua Caldera, New Zealand. *Geothermics, 21 (1–2)*. pp. 109–119. https://doi.org/10.1016/0375-6505(92)90072-H. (1992).

Land Information New Zealand: *Bay of Plenty 0.1m Urban Aerial Photos (2018–2019)* [data service]. https://data.linz.govt.nz/layer/104162-bay-of-plenty-01m-urban-aerial-photos-2018-2019/. Accessed 18/11/2020. (2019).

Milner, D., Cole, J., Wood, C.: Asymmetric, multiple-block collapse at Rotorua Caldera, Taupo Volcanic Zone, New Zealand. *Bulletin of Volcanology, 64*. pp 134–149. (2002).

Reeves, R.R., Scott, B.J., Hall, J.: *2014 thermal infrared survey of the Rotorua and Lake Rotokawa-Mokoia geothermal fields*. Lower Hutt (NZ): GNS Science. (GNS Science report; 2014/57). 24 p. (2014).

Scott, B.J., Mroczek, E.K., Burnell, J.G., Zarrouk, S.J., Seward, A.M., Robson, B., Graham, D.J.: Rotorua Geothermal Field: An experiment in environmental management. In: Chambefort, I. and Bignall, G., editors: *Taupo Volcanic Zone geothermal systems, New Zealand: Exploration, science and development*. Amsterdam (NL): Elsevier. pp. 294–310. (Geothermics; 59B). (2016).

Spichak, V. and Manzella, A. Electromagnetic sounding of geothermal zones. *Journal of Applied Geophysics, 68 (4)*. pp 459–478. https://doi.org/10.1016/j.jappgeo.2008.05.007. (2009).

Ratouis, T.M.P., O'Sullivan, M.J., Alcaraz, S.A., O'Sullivan, J.P.: The effects of seasonal variations in rainfall and production on the aquifer and surface features of Rotorua geothermal field. *Geothermics, 69*. pp 165–188. https://doi.org/10.1016/j.geothermics.2017.05.003. (2017)

Taylor, C.B. and Stewart, M.K.: Hydrology of Rotorua geothermal aquifer, New Zealand. *Proc. Int. Symp. Isotope Techniques in Water Resources Development*, Vienna. pp. 25–45. (1987).

Thompson, G.E.K.: *Near surface ground temperatures in the North Island volcanic belt*. Wellington (NZ): Department of Scientific and Industrial Research. Report 68. 15 p. (1971).

Wood, C.P.: 1992. Geology of the Rotorua Geothermal System. *Geothermics, 21 (1–2)*. pp 25–41. https://doi.org/10.1016/0375-6505(92)90066-I (1992).

Viezzoli, A., Auken, E., Munday, T.: Spatially constrained inversion for quasi 3D modeling of airborne electromagnetic data: An application for environmental assessment in the lower Murray region of South Australia. *Exploration Geophysics, 40 (2)*. pp. 173–183. https://doi.org/10.1071/EG08027. (2009).